Gas-Transport Properties of Ethylene/Propylene/Carbon Monoxide Polyketone Terpolymer

M. A. DEL NOBILE,[1] G. MENSITIERI,[1] L. NICOLAIS,[1,*] A. SOMMAZZI,[2] and F. GARBASSI[2]

Department of Materials and Production Engineering, University of Naples "Federico II," P.le Tecchio 80, 80125 Naples, Italy; Istituto Guido Donegani, via G. Fauser 4, 28100 Novara, Italy

SYNOPSIS

The demand for heat-stable and easily processable polymeric materials with good gas-barrier properties is becoming more and more important due to the advent of new technological applications in the field of food packaging. A renewed interest has arisen for a polyketone class of polymers, which seems to fulfill these requirements. Our attention has been focused on a polyketone terpolymer (0.93 : 0.07 : 1 ethylene/propylene/carbon monoxide) in order to determine the transport properties and to relate them to the polymer structure. Permeability tests have been performed at three different temperatures (25, 35, and 45°C) with three different gases (helium, oxygen, and carbon dioxide). Permeabilities, diffusivities, and solubilities have been evaluated. Their dependence on temperature was interpreted on the basis of permeation and diffusion apparent activation energies (E_p and E_d) and of heats of solution (ΔH_s). The investigated polymer has been found to be rubbery at the test temperature (glass transition temperature is about 17°C), but the detected permeabilities are comparable to those of glassy polymers widely used for packaging applications. The experimentally determined diffusion coefficients have been related to the semicrystalline nature of the polymer and to the different dimensions of the gas adopted in the investigation. The gas-solubility coefficients determined from permeability measurements were related to the force constant of the gas molecules in the Lennard-Jones (6–12) potential field equation. © 1993 John Wiley & Sons, Inc.

INTRODUCTION

Polyketones are attractive polymers to be used in food-packaging applications. This class of polymers is reported[1,2] to fulfill both processing and food-preservation requirements. In fact, they are one-step processable, have good impact properties, are dimensionally heat-stable, are easily compoundable with other polymers used for food packaging (nylon, polycarbonate, and ethylene vinyl alcohol copolymer), and, as will be discussed, have good barrier properties competitive with those of nylon and poly(ethylene terephtalate) (PET).

Olefins and carbon monoxide copolymerize with high conversions in the presence of Group VIII transition-metal compounds.[3] The catalyst systems typically include a Pd(II) salt in methanol in combination with bidentate phosphine or bidentate nitrogen ligand, an acid, and, optionally, an oxidant such as p-benzoquinone. The resulting copolymers, i.e., polyketones, are high melting solids, showing a regular structure with alternating CO and olefin units. The ethylene/carbon monoxide copolymer has a melting temperature (T_m) of approximately 257°C. To process the material, it must be heated to at least 25°C above the T_m. Since its thermal stability is too low to withstand such temperatures without decomposition, a 5–10% (mol) of a third monomer (e.g., propylene) can be introduced along the chain to overcome this deficiency. As the amount of propylene in the terpolymer increases, the T_m decreases and processing temperatures can be reduced below the decomposition temperature.

The polyketone investigated in the present study is a linear terpolymer consisting of alternating aliphatic and carbon monoxide groups, the aliphatic

---

group being either a polyethylene or polypropylene repeating unit, as shown below:

$$\left[\!\!\left(CH_2 - CH_2\right)\!\!- CO\right]_n \qquad \left[\!\!\left(P\right)\!\!- CO\right]_m$$
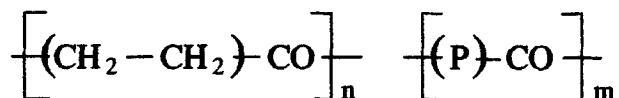
where "P" is the propylene unit and the ratio $m : n$ is about 0.07. The $-CO-(C_2H_4)-$ units and the $-CO-(P)-$ units occur randomly throughout the polymer backbone.

This material is a semicrystalline rubbery polymer at 25°C. The barrier properties are reported to depend on the cooling protocol of the manufacturer,[2] probably due to the different developed amount of crystallinity and to the different crystal shapes and dimensions.

In the present study, gas-permeation tests have been performed at different temperatures and pressures with several gases differing for dimensions and polarities (helium, oxygen, and carbon dioxide) on semicrystalline terpolymer samples showing 42% crystallinity.

The gas-permeation process in totally amorphous rubbery polymers can be described in terms of a dissolution–diffusion mechanism. Henceforth, in the examination of gas-transport properties, both the kinetic (diffusivity) and equilibrium (solubility) aspects need to be analyzed.

Generally, the solubility of simple gases in totally amorphous rubbery polymers does not change with pressure at low pressure levels. In these cases, the gas-sorption process can be described in terms of the simple Henry's law:

$$C = k^* \cdot p \qquad (1)$$

where C is the gas concentration in the polymer; p, the gas pressure; and k^*, the Henry's solubility constant.

The solubility process in semicrystalline rubbery polymers has been described[4–8] in terms of a "reduced solubility." In the case of semicrystalline rubbery polymers, it can be supposed that the amorphous fraction has characteristic thermodynamic properties that are independent of the level of crystallinity and that the crystalline phase does not dissolve any gas molecules. This assumption is supported by experimental results reported for several polymer–gas systems.[5,9,10] On this basis, we can express the semicrystalline gas solubility coefficient k as a function of the amorphous volumetric fraction

(α) and of the amorphous solubility coefficient (k^*) according to the following equation:

$$k = \alpha \cdot k^* \qquad (2)$$

A more complicated expression has to be used to relate the gas diffusivity of the totally amorphous rubbery polymer to that of the corresponding semicrystalline polymer. According to Michaels and Bixler,[6] this can be accomplished by using two parameters, τ and β, which are named, respectively, "tortuosity factor" and "immobilization factor." τ takes into account the fact that the presence of the impervious crystallites brings about an increase of the diffusive path length ("detour effect").[11] On the other hand, β embodies both the effect of crystallites on the segmental mobility of the polymer amorphous fraction and the "blocking effect," the latter being related to the thinness of amorphous layers.[11] As a consequence, the gas diffusivity in the semicrystalline polymer can be expressed by the following equation:

$$D = \frac{D^*}{\tau \cdot \beta} \qquad (3)$$

where D^* is the gas diffusivity in the totally amorphous polymer.

EXPERIMENTAL

Materials

Ethylene–propylene–CO terpolymer, used in the present study, was prepared with palladium catalyst, according to published procedures.[3] The resulting polymer (where the amount of the propylene–CO group is 7%, randomly distributed along the chain) is a white, highly crystalline solid with a limiting viscosity number (LVN) of 1.5 dL/g, measured in m-cresol at 100°C in a standard capillary viscosity measuring device. The glass transition temperature (T_g) is about 17°C and the melting point is about 220°C. Film samples of terpolymer (thickness = 0.2 mm) were produced by compression-molding, heating the terpolymer up to a temperature 20°C above its melting point and cooling slowly. The percentage of crystallinity, estimated from X-ray diffraction, is about 42%.

For the sake of comparison, oxygen permeability measurements were also performed on commercial films of poly(ethylene terephtalate) (PET) (*ICI*

"melinex," thickness = 0.012 mm) and nylon 6 (*SNIA Tecnopolimeri* nylon 6 "cast," thickness = 0.02 mm, and nylon 6 "bioriented," thickness = 0.025 mm). The gases used in the permeation measurements had a purity greater than 99.95% and were used without further purification.

Methods

Permeability tests were performed in a gas–membrane–gas configuration (dry conditions). A technique based on the detection of the pressure increase at the downstream side of the polymer film pressurized at the upstream side was used. The polymer sheet is located in a gas-tight permeation cell separating the upstream and downstream chambers. Before the permeation test, each sample was allowed to desorb moisture eventually absorbed in the material during storage, degassing both the chambers for several days at about 10^{-4} Torr. Prior to each test, the upstream side was pressurized with the gas under investigation while the downstream side was still at the degassing pressure. The value of the upstream gas pressure was measured by a pressure transducer with a full-scale range of 10 atm (Transinstruments BHL-4240 with an accuracy of 0.04% F.S.). A very sensitive pressure transducer with a full scale range of 10 Torr (M.K.S. Baratron 221A, with an accuracy of 0.5% of the reading) was used to monitor the pressure increase on the downstream side. On the downstream side, the pressure never exceeded 1/1000 of the upstream pressure during all the permeation tests. This was obtained through a proper adjustment of the downstream chamber volume as the gas under investigation was changed. The exact value of this volume was measured by gas-expansion techniques. The permeation apparatus was positioned in an air-circulating box, whose temperature controller is able to keep the apparatus at the set temperature with an accuracy of ±0.1°C. The volume (cm^3 [STP]) of gas penetrated through the polymer as function of time was evaluated from the downstream pressure values using the ideal gas law. In each experiment, enough time was allowed to ensure the attainment of steady-state permeation. The permeability was computed from the slope of the linear steady-state part of the curve representing the permeated gas volume as function of time. To evaluate the gas diffusivity, the "time lag" was determined from the intercept of the steady-state permeability curve on the abscissa.

Wide-angle X-ray diffractograms have been obtained in transmission using a powder diffractometer PW 1020 Philips. The CuKα radiation was used in the angular range 5°–60°. The raw spectra were further analyzed by the Graphic Mathematical Package with a Unisys 1100 mainframe computer (Instituto Guido Donegani/Unisys).

Crystallinity was calculated by subtracting the amorphous halo from the original diffractogram between 5° and 40° and calculating the respective area values by digital integration. The polymer was examined by transmission electron microscopy (TEM) using a Philips 300 instrument. The sample was prepared for observation by microtomy.

RESULTS AND DISCUSSION

The solubility and diffusivity coefficients were evaluated by permeability tests. The diffusivity was calculated from the "time-lag" value according to the following equation:

$$D = \frac{l^2}{6 \cdot \theta} \tag{4}$$

where l is the sample thickness, and θ, the measured time lag. The solubility coefficient has been determined as the ratio of detected permeability and diffusion coefficient, the latter being evaluated from eq. (4), i.e.:

$$k = \frac{P}{D} \tag{5}$$

where P is the measured gas permeability.

Equations (4) and (5) presume the validity of the Henry's law for gas sorption and of the first Fick's law with constant diffusivity for gas transport, which are reasonable assumptions in the case of gas permeation in rubbery semicrystalline polymers.

Table I reports the diffusivity, solubility, and permeability data obtained for helium, oxygen, and carbon dioxide at three different temperatures (25, 35, and 45°C). Table II reports the permselectivities for the three investigated gases. Permselectivities were simply evaluated from the ratio of the pure gas permeabilities (this ratio is generally reported as "ideal permselectivity"); this is reasonable because of the very low downstream pressure adopted and of the assumed negligible influence of one gas on the permeability of the other. Permeability measurements were performed at upstream gas pressures ranging from 0.1 to 0.4 MPa: The fluctuations of measured values of permeability and time lag at the different pressures investigated were in the limit of

Table I   Diffusivity, Solubility, and Permeability Data of Helium, Oxygen, and Carbon Dioxide for the Polyketone Terpolymer at 25, 35, and 45°C

Temperature (°C)	D $\left(\dfrac{cm^2}{s}\right)$	k $\left(\dfrac{cm^3\ (STP)}{cm^3 \cdot atm}\right)$	P $\left(\dfrac{cm^3\ (STP)\ cm}{cm^3 \cdot atm \cdot min}\right)$	Gas
25	$2.65 \cdot 10^{-6}$	0.00152	$2.35 \cdot 10^{-7}$	He
25	$6.04 \cdot 10^{-9}$	0.01390	$5.03 \cdot 10^{-9}$	O_2
25	$1.23 \cdot 10^{-9}$	0.58300	$4.41 \cdot 10^{-8}$	CO_2
35	$2.95 \cdot 10^{-6}$	0.00206	$3.65 \cdot 10^{-7}$	He
35	$1.04 \cdot 10^{-8}$	0.01740	$1.09 \cdot 10^{-8}$	O_2
35	$3.00 \cdot 10^{-9}$	0.54100	$9.58 \cdot 10^{-8}$	CO_2
45	$4.28 \cdot 10^{-6}$	0.00219	$5.63 \cdot 10^{-7}$	He
45	$1.64 \cdot 10^{-8}$	0.02440	$2.40 \cdot 10^{-8}$	O_2
45	$5.82 \cdot 10^{-9}$	0.52300	$1.90 \cdot 10^{-7}$	CO_2

apparatus' accuracy. Henceforth, the dependency of transport parameters on upstream pressure was neglected. The data reported were averaged over at least five measurements.

Oxygen permeability tests were also run on the same equipment with commercial nylon 6 and PET films. The detected oxygen permeability values for the investigated polyketone ($6.04 \cdot 10^{-9}$ expressed in the units adopted in Table I) at 25°C are lower than those measured for cast nylon 6 ($9.25 \cdot 10^{-9}$) and semicrystalline PET ($11.7 \cdot 10^{-9}$) and close to those detected for bioriented nylon 6 ($4.97 \cdot 10^{-9}$). The polyketone is characterized by low permeabilities and high permselectivities even when compared to that of glassy polymers like polycarbonate, polysulfone, and poly(phenylene oxide).[12]

Figures 1–3 report the Arrhenius' plots for gas permeabilities and diffusivities and the van't Hoff's plot for the solubility coefficient. In the investigated temperature range, the data are fairly well represented by a linear relationship relating the natural logarithm of the considered parameter to the reciprocal of absolute temperature. As a consequence, the dependence on temperature of diffusion, solubility, and permeability can be expressed as follows:

$$D = D_0 \cdot \exp\left(-\frac{E_d}{R \cdot T}\right) \qquad (6)$$

$$k = k_0 \cdot \exp\left(-\frac{\Delta H_s}{R \cdot T}\right) \qquad (7)$$

$$P = P_0 \cdot \exp\left(-\frac{E_p}{R \cdot T}\right) \qquad (8)$$

where E_d is the apparent activation energy related to the diffusion process; ΔH_s, the heat of solution; and E_p, the sum of E_d and ΔH_s. Table III reports the values of E_d, ΔH_s, and E_p.

Solubility

The natural logarithm of solubility coefficients referred to the amorphous phase (k^*) determined by eqs. (5) and (2) at different temperatures shows a roughly linear behavior if reported as function of ε/k, the force constant in the Lennard-Jones (6–12) potential field equation, as displayed in Figure 4. This kind of relationship, as proposed by Michaels and Bixler,[5] is based on the analogy between the penetrant dissolution process in a rubbery amor-

Table II   Permselectivities for the Polyketone Terpolymer at 25, 35, and 45°C

Temperature (°C)	$S_{He/O_2} = \dfrac{P_{He}}{P_{O_2}}$	$S_{He/CO_2} = \dfrac{P_{He}}{P_{CO_2}}$	$S_{CO_2/O_2} = \dfrac{P_{CO_2}}{P_{O_2}}$
25	46.8	5.33	8.80
35	33.5	3.81	8.80
45	23.5	2.97	7.94

Figure 1 Natural logarithm of permeability vs. reciprocal of the absolute temperature for helium, oxygen, and carbon dioxide.
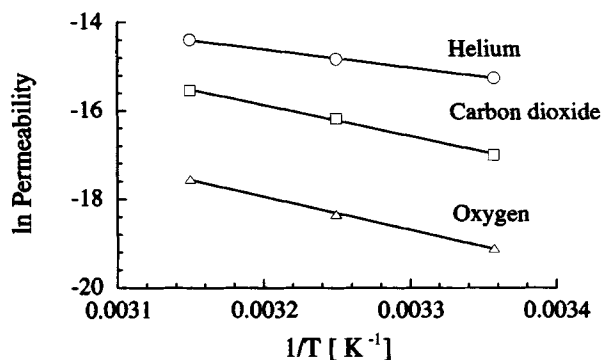

Figure 3 Natural logarithm of solubility vs. reciprocal of the absolute temperature for helium, oxygen, and carbon dioxide.

phous polymer and in a low molecular weight nonpolar liquid. The thermodynamic assumptions that underlie this relationship seem to be rather supported, in our case, by the experimental results.

Diffusivity

As anticipated in the Introduction, the proper analysis of the gas-diffusion process in a semicrystalline polymer must be analyzed in terms of "tortuosity" (τ) and "immobilization" (β) factors. Following the approach proposed by Michaels and Bixler[6] to interpret the gas flow in semicrystalline polyethylene, the values of D^*, τ, and β were approximately estimated.

According to this approach, the diffusivities must be correlated to a "reduced molecular diameter" defined by the equation
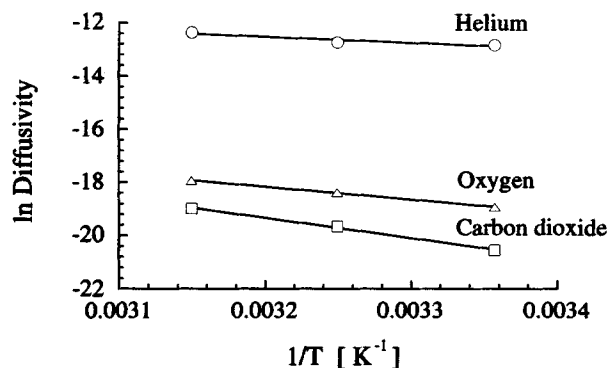
$$d' = d - \frac{\sqrt{\phi}}{2} \qquad (9)$$

Figure 2 Natural logarithm of diffusivity vs. reciprocal of the absolute temperature for helium, oxygen, and carbon dioxide.
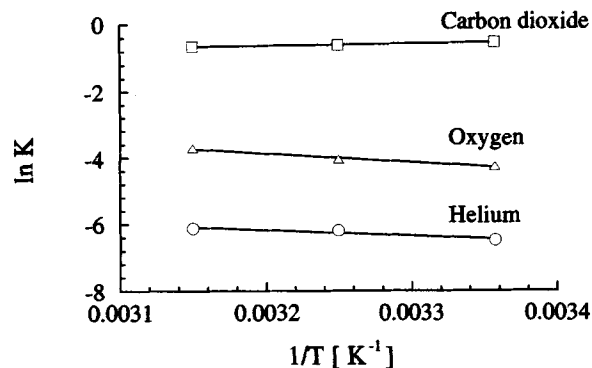
where ϕ is the free volume per unit length of the monomeric group measured along the chain axis or, alternatively, $\phi^{1/2}/2$ is approximately equal to the mean unoccupied distance between two chain segments and d is the diffusant diameter.

The activation energy for gas diffusion can be split in two distinct contributions as proposed by Brandt[13]: (a) intermolecular energy related to chain-segment separation and (b) the intramolecular energy due to the bending of the polymer backbone. Assuming that the carbon monoxide group does not decrease appreciably the flexibility of the aliphatic segments involved in a diffusional jump, it is possible to neglect the bending energy contribution to the activation energy, following the arguments presented by Michaels and Bixler[6] for polyethylene. On these bases, they proposed the following relationship of D^* with the "reduced molecular diameter" that we used also in our analysis:

$$\ln\left(\frac{D^*}{d^2}\right) = a + b \cdot [d - (\sqrt{\phi}/2)] \qquad (10)$$

Table III Permeation and Diffusion Apparent Activation Energies (E_P and E_D) and Heats of Solution (ΔH_S), for Helium, Oxygen, and Carbon Dioxide at 25, 35, 45°C

Gas	E_P $\left(\dfrac{\text{kcal}}{\text{mol}}\right)$	E_d $\left(\dfrac{\text{kcal}}{\text{mol}}\right)$	ΔH_S $\left(\dfrac{\text{kcal}}{\text{mol}}\right)$
He	8.147	4.569	3.157
O_2	14.437	9.220	5.218
CO_2	13.690	14.697	−1.013

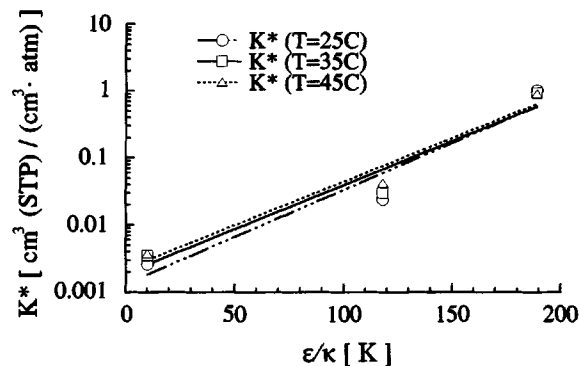**Figure 4** Logarithmic plot of totally amorphous polymer gas solubilities vs. the Lennard-Jones potential well-depth parameter of gas.

Figure 5 TEM micrograph of terpolymer spherulitic structures (magnified 14,400 times).

Moreover, the following empirical equation was assumed[6] to hold true for β, based on arguments related to the entropy of activation:

$$\ln \beta = c \cdot [d - (\sqrt{\phi}/2)]^2 \qquad (11)$$

Subtracting eq. (11) from eq. (10), one obtains

$$\ln \frac{D^*}{d^2 \cdot \beta} = a + b \cdot [d - (\sqrt{\phi}/2)]$$
$$- c \cdot [d - (\sqrt{\phi}/2)]^2 \qquad (12)$$

The values of a, b, and c can be evaluated from a parabolic fit of the natural logarithm of the group $D^*/ (d^2 \beta)$ plotted as function of the "reduced molecular diameter."

Based on the terpolymer density data, on the estimated crystallinity, and on the calculated density of the crystal, the value of $\phi^{1/2}/2$ has been estimated to be equal to 0.876 Å. To calculate the density of the crystal, the crystal structure was assumed to be identical to that of the 1 : 1 ethylene/carbon monoxide copolymer,[14] due to the neglectable amount of propylene moiety present in the backbone.

The similarity of terpolymer crystal macrostructure to that of polyethylene, as observed by TEM photomicrographs reported in Figure 5, motivated the estimation of the value of the terpolymer tortuosity factor (τ) by means of the nth power law relationship suggested by Michaels and Bixler,[6] using for n the value they adopted in the case of linear polyethylene prepared from Phillips catalysts (n = 1.25). We estimated for our samples a value of 1.85 for the tortuosity factor.

Using both the value determined for τ and the experimental values of D, it was possible to calculate
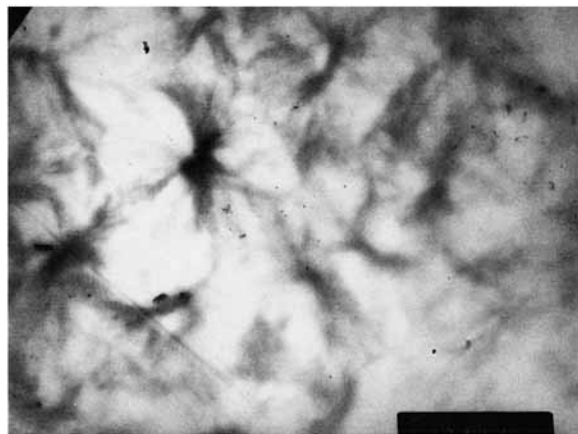
the ratio D^*/β for the different gases from eq. (3). Figure 6 reports the plot of the natural logarithm of the group $D^*/ (d^2 \beta)$ as function of d' at 25°C. It is to be noted that in this correlation a correction of the helium molecular diameter was introduced, as suggested by Michaels and Bixler,[6] in order to take into account that an appreciable amount of non-activated diffusion could occur for helium. The correction factor (2.5) proposed for polyethylene[6] was adopted in this investigation.

Using a parabolic fit of data reported in Figure 6, it was possible to evaluate the constants appearing in eq. (12), i.e., a, b, and c. The curvature shown is extremely small and thus sensitive to small errors in the calculated values of $D^*/ (d^2 \beta)$. As a consequence, only crude estimates of the these constants, and, hence, of D^* and β, were obtained. Table IV reports the values obtained for D, D^*, and β in the case of terpolymer and, for comparative purposes,
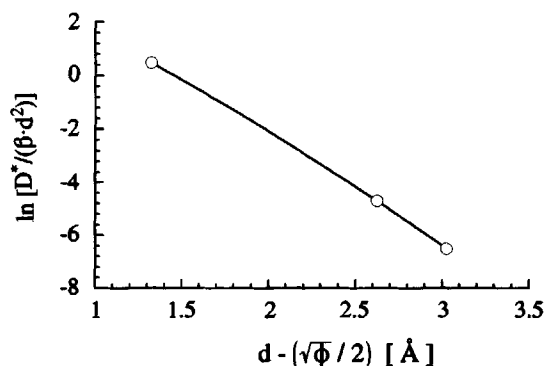

Figure 6 Plot of the natural logarithm of the group $D^*/ (d^2 \beta)$ as a function of d' at 25°C.

Table IV   Totally Amorphous Polymer Gas Diffusivities (D^*), Immobilization Factor (β), and Gas Diffusivities of the Helium, Oxygen, and Carbon Dioxide at 25°C, for Both the Polyketone Terpolymer and the Polyethylene

Gas	D $\left(\dfrac{cm^2}{s}\right)$	D^* $\left(\dfrac{cm^2}{s}\right)$	β	Polymer
He	$2.65 \cdot 10^{-6}$	$8.46 \cdot 10^{-6}$	1.73	Terpolymer
He	$3.07 \cdot 10^{-6}$	$2.16 \cdot 10^{-5}$	1.10	Polyethylene[a]
O_2	$6.04 \cdot 10^{-9}$	$9.58 \cdot 10^{-8}$	8.59	Terpolymer
O_2	$1.70 \cdot 10^{-7}$	$1.74 \cdot 10^{-6}$	1.60	Polyethylene[a]
CO_2	$1.23 \cdot 10^{-9}$	$3.76 \cdot 10^{-8}$	17.40	Terpolymer
CO_2	$1.24 \cdot 10^{-7}$	$1.27 \cdot 10^{-6}$	1.60	Polyethylene[a]

[a] The data for polyethylene were taken from Ref. 6 and refer to a polyethylene with a crystallinity level of 0.77 and a tortuosity factor of 6.4 (in Ref. 6, the polyethylene was referred as Grex).

of polyethylene. Although the reliability of the reported values for D^* and β is affected by the accuracy of the curve fitting shown in Figure 6, few comments can be made. The low gas diffusivities (D) of the terpolymer compared to that of the polyethylene can be ascribed both to the reduced segmental mobility proper of the totally amorphous polymer (lower value of D^*) and to a strong blocking effect due to the presence of crystals (higher value of β). On the other hand, the terpolymer gas solubility is about half of the value generally reported for polyethylene, suggesting that the low permeabilities detected for the terpolymer stem mainly from the lower polymer segmental mobility (lower gas diffusivity) rather than from the lower gas solubility.
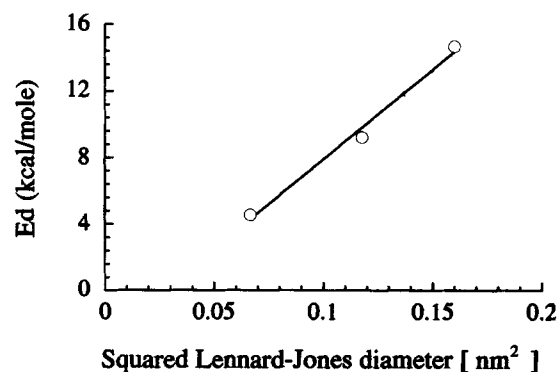
Activation Energies

Several molecular theories have been developed in order to predict the dependence of the apparent activation energy on the gas molecular shape and dimension[13,15–20] and have been applied to both totally amorphous[17,19] and to semicrystalline polymers.[19] Various functional forms have been proposed depending on the adopted theoretical interpretation of the activated diffusion process. For many polymer/simple gas systems, the dependency of the apparent activation energy on the gas molecular diameter has been empirically factored in the product of two functions,[21,22] one characterizing the polymer and the other related to the gas diameter. The dependency of the apparent activation energy on the gas diameter has been reported to be linear or quadratic depending on the polymer–penetrant system.[23] Because of the limited range of investigated temperatures and the unavailability of the appro-

priate model parameters characterizing the polymer structure, no attempt was made to use any of the mentioned models in the case of the present data. Nevertheless, a semiempirical approach to the interpretation of the diffusion process is possible.

Figure 7 reports the apparent activation energy as function of the squared Lennard-Jones diameter. In the investigated range of examined diameters, an approximately linear dependence of E_d on the squared Lennard-Jones diameter has been detected. This linear correlation is close to the ideas developed by Meares,[15] who interpreted the activation energy as the energy required to open a cylindrical passageway according to the equation

$$E_d = (\pi/4) \cdot d_G^2 \cdot l_D \cdot CED \qquad (13)$$

where l_D is the length of the cylindrical passageway; d_G, the diffusant collision diameter; and CED, the

Figure 7   Plot of apparent diffusion activation energy vs. squared Lennard-Jones diameter of gas.

polymer cohesive energy density. The more physically reasonable interpretations proposed by Pace and Datyner[18,19] and by DiBenedetto[16] both predict a downward concavity of E_d expressed as a function of the penetrant diameter in the first case and expressed as a function of the squared penetrant diameter in the second case. However, the range of the diffusant molecular diameter examined in this investigation is too limited to evidence these behaviors.

CONCLUSIONS

Gas-permeation measurements performed on an ethylene/propylene/carbon monoxide (0.93/0.07/1) polyketone terpolymer with different gases (He, O_2, CO_2) have shown good barrier properties as well as good selectivities notwithstanding the fact that the test temperatures were above the polymer glass transition temperature.

In the range of investigated temperatures, permeability, solubility, and diffusivity data were successfully correlated by Arrhenius-type relationships.

The low gas permeabilities of the investigated polyketone terpolymer compared to polyethylene stem mainly from the substantially lower value of diffusivities rather than from the slightly lower gas solubilities. The low diffusivity values seem to be due both to a higher value of the so-called immobilization factor (greater β) related to the semicrystalline nature of the polymer and to a lower intrinsic segmental mobility of the amorphous fraction (smaller D^*).

REFERENCES

1. W. H. Korcz, J. R. Kastelic, K. C. Dangayach, and T. A. Armer, Eur. Pat. 0, 306, 115, A2 (Sept. 2, 1988).
2. L. E. Gerlowski and J. R. Kastelic, U.S. Pat. 5,077,385 (Dec. 31, 1991).
3. E. Drent, Eur. Pat. Appl. 121,965 (1984) and 181,014 (1986). J. A. M. van Broekhoven, E. Drent, and E. Klei, Eur. Pat. Appl. 213,671 (1987).
4. A. S. Michaels and R. B. Parker, Jr., *J. Polym. Sci.*, **41**, 53 (1959).
5. A. S. Michaels and H. J. Bixler, *J. Polym. Sci.*, **50**, 393 (1961).
6. A. S. Michaels and H. J. Bixler, *J. Polym. Sci.*, **50**, 413 (1961).
7. W. J. Koros and M. W. Hellums, in *Encyclopedia of Polymer Science and Engineering*, Supplement Vol., H. F. Mark, N. M. Bikales, C. G. Overberger, G. Menges, and J. I. Kroschwitz, Eds., Wiley, New York, 1990.
8. C. H. Klute, *J. Appl. Polym. Sci.*, **1**(3), 340 (1959).
9. H. J. Bixler and O. J. Sweeting, in *The Science and Technology of Polymer Films*, O. J. Sweeting, Ed., Wiley, New York, 1971, Vol. 2.
10. J. Crank and G. S. Park, *Diffusion in Polymers*, Academic Press, New York, 1968.
11. A. Peterlin, *J. Macromol. Sci.-Phys.*, **B11**(1), 57 (1975).
12. R. R. Zolandz and G. K. Fleming, in *Membrane Handbook*, W. S. W. Ho and K. K. Sirkar, Eds., Van Nostrand Reinhold, New York, 1992, Part II, Chap. 3, p. 25.
13. W. W. Brandt, *J. Phys. Chem.*, **63**, 1080 (1959).
14. Y. Chatani, T. Takizawa, S. Murahashi, Y. Sakata, and Y. Nishimura, *J. Polym. Sci.*, **55**, 811 (1961).
15. P. Meares, *J. Am. Chem. Soc.*, **76**, 3415 (1954).
16. A. T. DiBenedetto, *J. Polym. Sci. Part A*, **1**, 3477 (1963).
17. D. R. Paul and A. T. DiBenedetto, *J. Polym. Sci. Part C*, **10**, 17 (1965).
18. R. J. Pace and A. Datyner, *J. Polym. Sci. Polym. Phys. Ed.*, **17**, 437 (1979).
19. R. J. Pace and A. Datyner, *J. Polym. Sci. Polym. Phys. Ed.*, **17**, 453 (1979).
20. R. J. Pace and A. Datyner, *J. Polym. Sci. Polym. Phys. Ed.*, **17**, 465 (1979).
21. H. L. Frisch, *J. Polym. Sci. Part B*, **1**, 581 (1963).
22. T. K. Kwei and W. M. Arnheim, *J. Polym. Sci. Part A*, **2**, 957 (1964).
23. H. L. Frisch and T. K. Kwei, *J. Polym. Sci. Part B*, **7**, 789 (1969).